Available online at www.sciencedirect.com
SCIENCE DIRECT®
Acta Materialia 52 (2004) 1397–1408
Acta MATERIALIA
www.actamat-journals.com

# Void growth by dislocation emission

V.A. Lubarda [a,*], M.S. Schneider [a], D.H. Kalantar [b], B.A. Remington [b], M.A. Meyers [a]

[a] Department of Mechanical and Aerospace Engineering, University of California, San Diego, 9500 Gilman Drive, La Jolla, CA 92093-0411, USA
[b] Lawrence Livermore National Laboratories, Livermore, CA 94550-9234, USA

Received 4 June 2003; received in revised form 24 November 2003; accepted 25 November 2003

**Abstract**

Laser shock experiments conducted at an energy density of 61 MJ/m$^2$ revealed void initiation and growth at stress application times of approximately 10 ns. It is shown that void growth cannot be accomplished by vacancy diffusion under these conditions, even taking into account shock heating. An alternative, dislocation-emission-based mechanism, is proposed for void growth. The shear stresses are highest at 45° to the void surface and decay with increasing distance from the surface. Two mechanisms accounting for the generation of geometrically necessary dislocations required for void growth are proposed: prismatic and shear loops. A criterion for the emission of a dislocation from the surface of a void under remote tension is formulated, analogous to Rice and Thomson's criterion for crack blunting by dislocation emission from the crack tip. The critical stress is calculated for the emission of a single dislocation and a dislocation pair for any size of initial void. It is shown that the critical stress for dislocation emission decreases with increasing void size. Dislocations with a wider core are more easily emitted than dislocations with a narrow core.


*Keywords:* Voids; Vacancy diffusion; Dislocation emission; Laser; Shock

## 1. Introduction

The study of the nucleation and growth of voids in ductile metals is of significant interest for the understanding of failure under overall tensile loading. Such failure, for example, can occur upon reflection of tensile waves from a free surface of the shock-compressed plate. The growth and coalescence of voids in the vicinity of the back side of the plate can lead to spalling of the plate, with planar separation of material elements parallel to the wave front (e.g. [1–3]). Understanding material failure by void growth under dynamic loading conditions leading to spalling is an essential aspect of the design analysis of structures potentially targeted by explosive or projectile impacts. Extensive analytical and computational research has been devoted to analyze ductile void growth and coalescence in various materials and under various loading conditions. Representative references include [4–21]. Dynamic expansion of spherical cavities in elastoplastic metals was studied by Hopkins [22], Carroll and Holt [23], Johnson [24], Cortés [25], Ortiz and Molinari [26], Benson [27], Wang [28], Wu et al. [29], and others. The void nucleation and growth in nonlinear hyperelastic materials was analyzed by Williams and Schapery [30], Ball [31], Stuart [32], Horgan [33], and Polignone and Horgan [34], among others. A review by Horgan and Polignone [35] can be consulted for further references. With the exception of Cuitiño and Ortiz [18], these are all continuum treatments and are not explicitly based on specific mass transport (glide and/or diffusion) mechanisms. There is one dislocation model for void growth, proposed by Stevens et al. [36], but with some fundamental inconsistencies with it, pointed out by Meyers and Aimone [1]. Recently, there has also been a significant progress in the study of void nucleation, growth and coalescence by using the atomistic simulations (e.g. [37,38]).

The contribution in this paper has three goals:

(a) To present the results of laser-induced shock experiments in which the shock wave is allowed to reflect at a free surface, creating tensile pulses with a duration on the order of 10 ns.

* Corresponding author. Tel.: +1-858-534-3169; fax: +1-858-534-5698.
*E-mail address:* vlubarda@ucsd.edu (V.A. Lubarda).

1359-6454/$30.00 
doi:10.1016/j.actamat.2003.11.022

(b) To show that a diffusional mechanism of void growth cannot account for the growth process under high strain-rate tension loading, produced by the reflection of a shock wave at a free surface.
(c) To propose an alternative mechanism of void growth, by dislocation emission from the surface of the void. It will be analytically shown, for a two-dimensional configuration, that the imposed stresses in the laser shock experiments are sufficient for emitting dislocations from the void surface. The critical stress for the dislocation emission is found to decrease with an increasing void size, so that less stress is required to emit dislocations from larger than smaller voids.

## 2. Void formation in laser-driven shock experiments

Cylindrical specimens of monocrystalline copper, oriented to [0 0 1], were subjected to high tensile stresses during time intervals of tens of nanoseconds. This was accomplished by producing an ultra short shock wave by an incident laser beam with energies of 14, 41, and 61 MJ/m$^2$. The laser experiments conducted produce the shortest high-amplitude tensile pulses possible. This is orders of magnitude lower than explosives or plate-impact experiments. The shock wave was allowed to reflect as a tensile pulse from the rear free surface of the specimen. An approximate shape of the compressive pulse, as it propagates through the specimen and undergoes attenuation, is shown in Fig. 1. The specimen was about 1 mm thick. The initial peak pressure was of the order of 60 GPa, which decayed during the propagation through the sample in an approximately exponential manner. The experimental set-up and shock conditions is described by Meyers et al. [39] and Kalantar et al. [40].

The single crystal samples were encased in a recovery capsule. The assembly was recovered after shock and prepared for optical, scanning, and transmission electron microscopy. Experiments were conducted at different laser energy levels. The 61 MJ/m$^2$ experiment yielded spall initiation. Experiments at higher energy levels provided complete spalling and separation. Fig. 2 shows SEM images of (a) the initial specimen and (b) the recovered specimen with the bulged top surface. The laser was applied to the lower surface. The reflected tensile pulse at about 100 μm from the rear surface can be calculated from the decay of the shock pulse shown in Fig. 1. It is equal in magnitude, but opposite in sign, to the shock pressure. The latter is about 5 GPa in magnitude. The presence of the bulge in Fig. 2(b) demonstrates that the spall strength was exceeded. The images shown in Figs. 3(a) and (b) are taken from a longitudinal cut through the central axis of the cylindrical specimen. They were taken near the spall plane in order to examine the size and geometry of voids in the damaged region. Two magnifications are shown. The observed voids ranged in size from small voids (25–50 nm) to large voids (1 μm size).

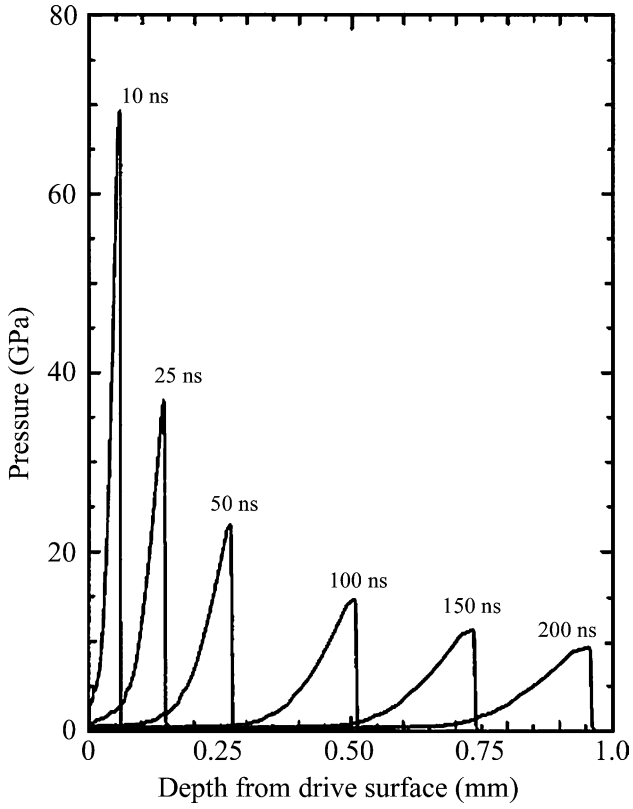


Fig. 1. Attenuation of the pressure pulse along the specimen thickness corresponding to a laser beam energy of 61 MJ/m$^2$.

The TEM image of a single crystal copper shocked to a 61 MJ/m$^2$ energy level is shown in Fig. 4(a). It reveals a dislocation cell structure, with a high dislocation density, of the order of $10^{15}$ m$^{-2}$ [39]. Fig. 4(b) shows what is believed to be a void near the back surface of the shocked specimen. Its diameter is approximately 0.5 μm. It may be argued that electropolishing produced the void, but a larger number of perforations were found close to the back surface of the specimen, where void formation is expected. There is a light rim around the void, indicating an extremely high dislocation density, beyond the point where individual dislocations can be imaged. This void is very similar to one observed earlier by Christy et al. [41] using high-voltage transmission electron microscopy. In that experiment the foil was not perforated and the same intense dislocation density was observed. Calculations demonstrate that the dislocation density around a void is extremely high. The diameter of this work-hardened layer is approximately twice the void diameter. Thus, a much higher dislocation density characterizes the region surrounding the void compared to regions without observable voids.

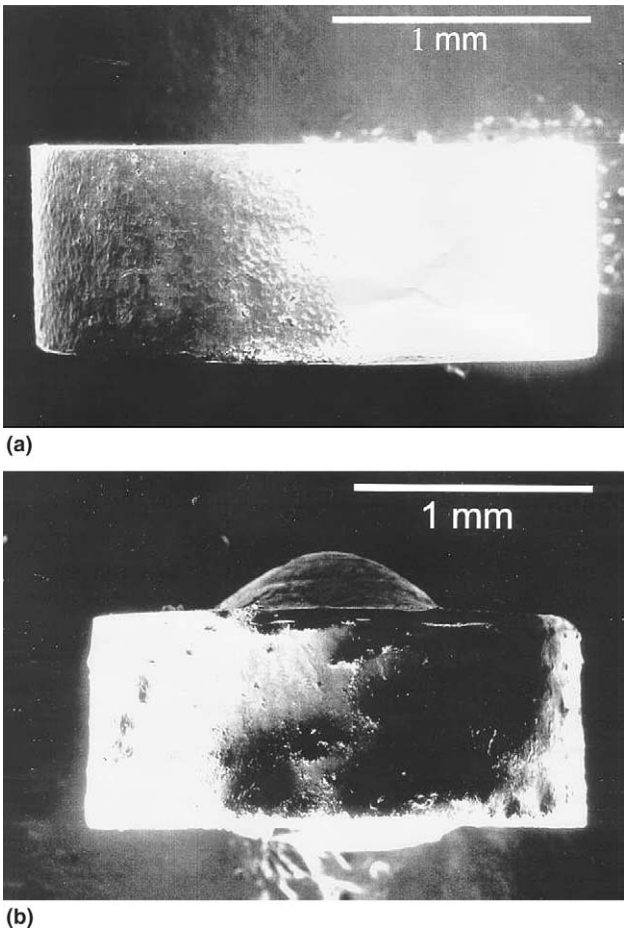


Fig. 2. Side view of the cylindrical specimen subjected to shock compression and subsequent reflected tension pulse from the laser-induced shock wave: (a) undeformed specimen and (b) deformed specimen (laser impulse applied to bottom surface) upon wave reflection with a spall surface (top).

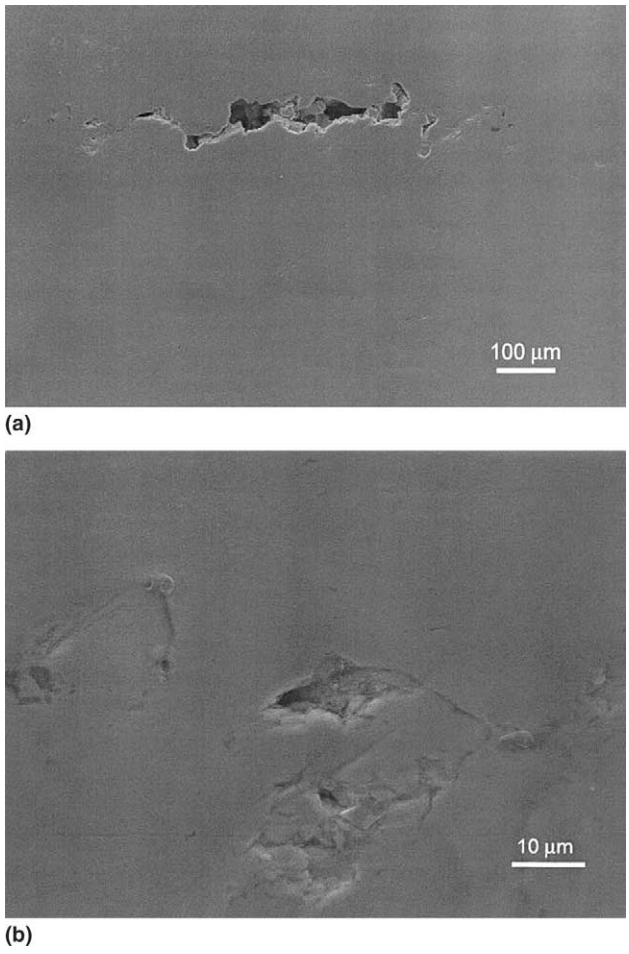


Fig. 3. SEM micrographs of voids at two length scales: (a) 100 μm and (b) 10 μm. Dark round areas represent voids.

## 3. Void growth by vacancy diffusion

Fracture by void nucleation, growth, and coalescence in ductile materials occurs at strain rates ranging from $10^{-5}$ to $10^{8}$ $s^{-1}$, so that different mechanisms of void growth can operate at different strain rate regimes. Cuitiño and Ortiz [18] proposed a vacancy diffusion mechanism for the nucleation of voids in single crystals, which is applicable in the range of low to moderate strain rates. The feasibility of void nucleation and growth by the vacancy diffusion mechanism is examined hereby taking into account the temperature rise due to shock compression. This temperature rise is in the range of several hundreds of degrees, depending on the peak shock pressure (Fig. 5(a)). The dominating diffusion mechanism is the pipe diffusion along the cores of dislocations (the lattice diffusion being negligible at these temperatures). The diffusion coefficient at the absolute temperature $T$ and for a reference dislocation density $\rho_0$ is $D(\rho_0) = D_0 \exp(-Q/kT)$, where $k$ is the Boltzmann constant, $Q$ is the activation energy of the pipe diffusion mechanism, and the pre-exponential factor $D_0$ is the experimentally determined or estimated coefficient. The reference dislocation density $\rho_0$ is the dislocation density of an undeformed material, which is typically in the range of $10^{10}$–$10^{12}$ $m^{-2}$. For copper, at this dislocation density, the coefficient $D_0$ is about $10^{-6}$ $m^2/s$, while $Q = 1.26$ eV [42]. Since the passage of the shock dramatically increases the dislocation density, and thus significantly enhances the pipe diffusion process, the diffusion coefficient is scaled by the ratio of the dislocation densities $\rho/\rho_0$, such that $D(\rho) = (\rho/\rho_0)D(\rho_0)$. For a laser energy density of 61 $MJ/m^2$ and shock pressure of 60 GPa, the residual temperature rise after the passage of the shock wave is about 600 K, with a corresponding dislocation density of about $10^{15}$ $m^{-2}$ [39]. Consequently, the effective diffusion coefficient is $D(\rho) = 3.57 \times 10^{-12}$ $m^2/s$.

Following Cuitiño and Ortiz [18], consider the vacancy diffusion process in the stage of steady state. For void growth to take place, there must be a net flux of vacancies into the void. By assuming a spherical void shape, and isotropic diffusion coefficients, the vacancy

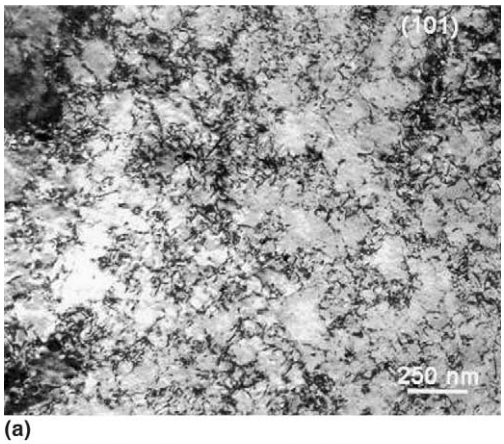


(a)

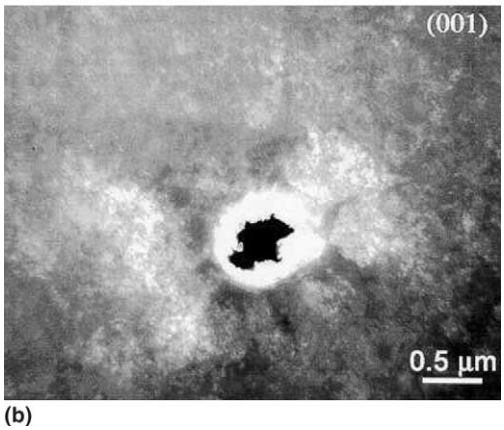


(b)

Fig. 4. TEM micrographs of laser-shocked monocrystalline copper: (a) bright field image of a high dislocation density with dislocation cell structure and (b) dark field image of an isolated void near the rear surface of the specimen and associated work-hardened layer (white rim).

flux into the void causes an increase of the current void radius $R$, which is governed by the differential equation

$$\frac{\mathrm{d}R}{\mathrm{d}t} = \frac{1}{R} D(c_0 - c_\mathrm{s}). \tag{1}$$

The initial and the equilibrium vacancy concentrations at the surface of the void are $c_0$ and $c_\mathrm{s}$, respectively. In the limiting case when the initial vacancy concentration $c_0$ is much larger than the equilibrium concentration at the surface of the void ($c_\mathrm{s} \ll c_0$), Eq. (1) can be integrated explicitly to give

$$\frac{R}{R_0} = \left(1 + \frac{2Dc_0}{R_0^2} t\right)^{1/2}. \tag{2}$$

In the calculations, the size of an initial vacancy cluster (void embryo) is taken to be $R_0 = 0.6$ nm, and the initial void concentration $c_0 = 10^5$. The nucleation stage ($R = 0$–$0.6$ nm) is not addressed here. It should be mentioned that shock compression generates vacancy concentrations that are three to four times the ones generated by low-strain rate plastic deformation to the same strain [43–45]. Thus, vacancy complexes (di, tri, tetravacancies, etc.) are present and can provide the initiation sites. Fig. 5(b) shows the calculated void size, assuming a Cuitiño–Ortiz diffusion mechanism, as a function of time. The calculations are conducted for three temperatures: 400, 600, and 900 K. The pressure in the back surface of the laser-driven experiments is approximately 5–10 GPa, providing a shock temperature rise of 40 K ($T = 340$ K). The temperature rise at the impact surface is 600 K ($T = 900$ K; $P = 60$ GPa). The temperature during the release portion is the residual temperature, much lower than the shock temperature. Thus, the shock temperature is a highly conservative estimate. A plot of the void size vs. time, shown in Fig. 5(b) and corresponding to Eq. (2), indicates that voids are unable to nucleate and grow by diffusion in the times created by lasers. For 900 K, the time required to grow a void to 30 nm is $10^{-3}$ s. At 600 K, it is 10 s. At 400 K they are not able to grow by diffusion at all. The critical void size beyond which the void is considered to be sufficiently large to grow by conventional macroscopic plasticity was defined to be of the order of an average dislocation spacing ($\rho^{-1/2}$), which is about 30 nm. Since available time in the shock loading of copper was of the order of tens of nanoseconds, the diffusion mechanism of void growth cannot take place. It is concluded that the considered pipe diffusion mechanism cannot operate at these extreme high strain rates.

This implies that an alternative mechanism of void growth must operate during the high strain-rate tension following laser-induced shock loading. This motivated our analysis presented in subsequent sections, in which a mechanism of void growth by the emission of dislocations from the surface of the void is proposed.

## 4. Void formation by dislocation emission

If vacancies cannot account for the growth of voids, dislocations need to be involved. Void growth is indeed a non-homogeneous plastic deformation process. The plastic strains decrease with increasing distance from the void center. The far-field strains are purely elastic, whereas plastic deformation occurs in the regions adjoining the surface of the void. Ashby [46] developed a formalism for the treatment of a non-homogeneous plastic deformation by introducing the concept of the generation of geometrically necessary dislocations. Two different mechanisms were envisaged by Ashby [46], based on prismatic or shear loop arrays.

The void growth situation is quite different from the rigid-particle model used by Ashby [46]. Nevertheless, it is still possible to postulate arrays of line defects to account for the non-homogeneous plastic deformation. Of critical importance is the fact that the shear stresses at 45° to the void surface are maximum, since the normal

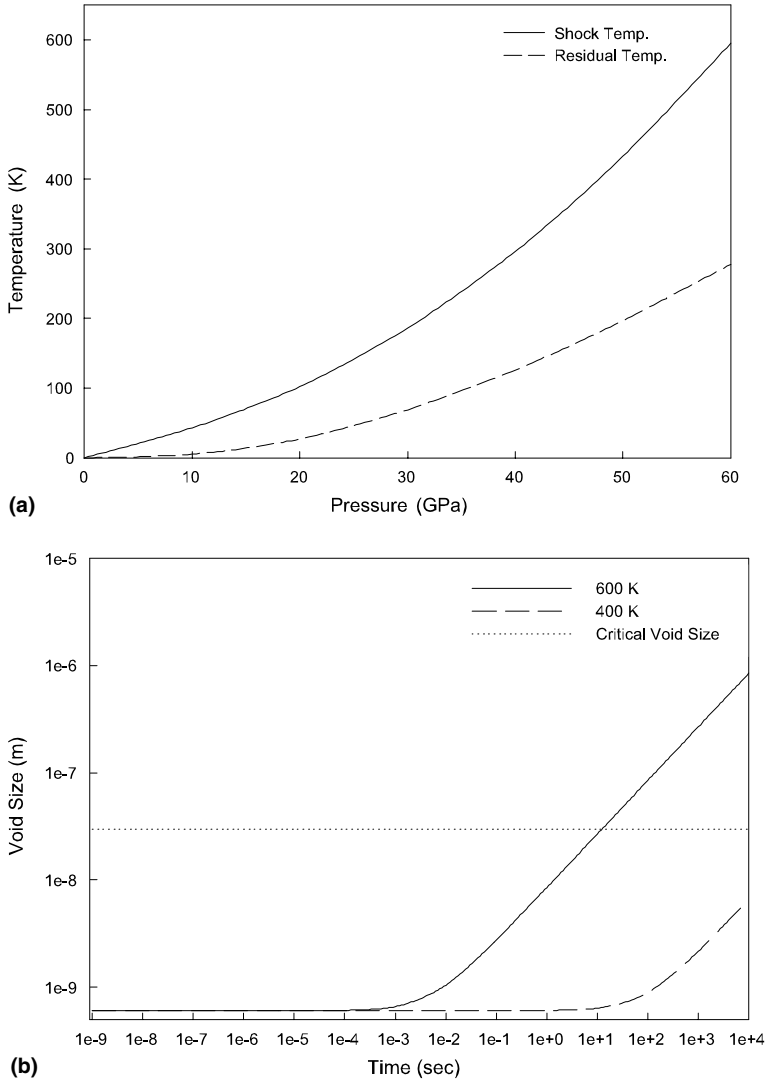


Fig. 5. (a) Temperature rise in copper due to laser-induced shock at different levels of pressure. Dashed curve represents shock temperature; solid curve is the residual temperature rise after the passage of the shock pulse. (b) Predicted void size as a function of time according to Eq. (2). The two curves correspond to two indicated temperature levels. The critical void size of about 30 nm is calculated from an average dislocation spacing corresponding to dislocation density in shock compression ($10^{15}$ m$^{-2}$).

stresses $\sigma_r$ are zero at the surface of the void. These shear stresses decay to zero at large distances due to the assumption of a far-field hydrostatic stress state. Thus, the shear stresses are highest at the internal surface, obviating dislocation nucleation there. The mechanisms of void growth by the emission of prismatic or shear loops will be considered here.

The mechanism of plastic deformation by *prismatic loop* emission is depicted in Fig. 6(a). A prismatic dislocation loop of radius $R/\sqrt{2}$ is punched out from a spherical void of radius $R$. This carries away a spherical sector causing an increase of the void's volume by an amount equal to $\pi R^2 b/2$. The *shear loop* mechanism involves the emission of dislocations along the slip plane, and is shown in Fig. 6(b). As in the case of the prismatic loops, these loops form preferentially at a plane intersecting the void along a 45° orientation to the radius. This ensures a 45° between the slip plane and the void surface, maximizing the driving force on the dislocation. The difference between this and the Ashby [46] loops is that the two opposite loops have dislocations of the same sign. Fig. 7(a) shows a top view of the *calota* (intersection of void with slip planes); four loop families are shown to illustrate the three-dimensional nature of the process. The center parts of the loops have edge character, while the regions close to the void surface have screw character. Cross-slip is expected to eventually occur and is schematically illustrated in Fig. 7(b). The activation of two cross-slip planes is shown.

In the two-dimensional case, four pairs of edge dislocations emitted from the surface of a cylindrical void under remote uniform tension give rise to an increase of

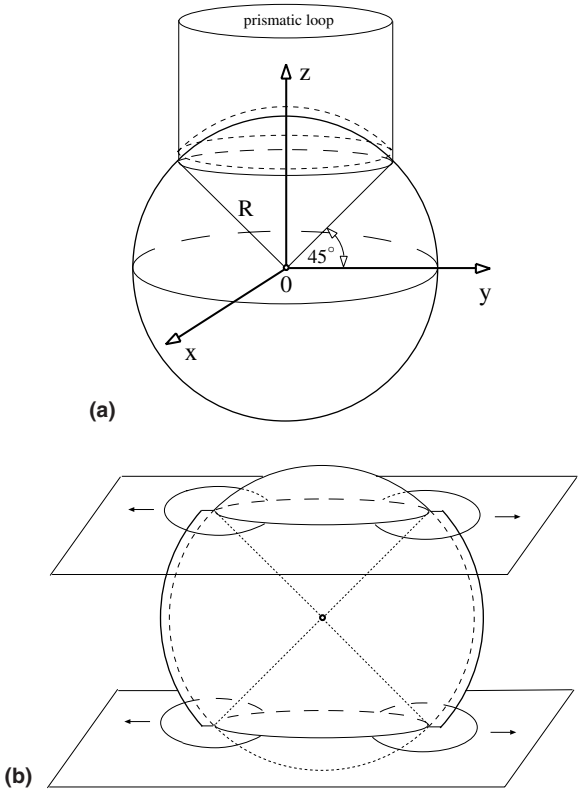


Fig. 6. (a) A prismatic dislocation loop of radius $R/\sqrt{2}$ punched out from a spherical void of radius $R$. The loop carries away the spherical sector (*calota*) causing an increase of the void's volume by an amount equal to $\pi R^2 b/2$. (b) Three-dimensional illustration of the emission of two pairs of dislocation shear loops from the void surface along the indicated slip planes.

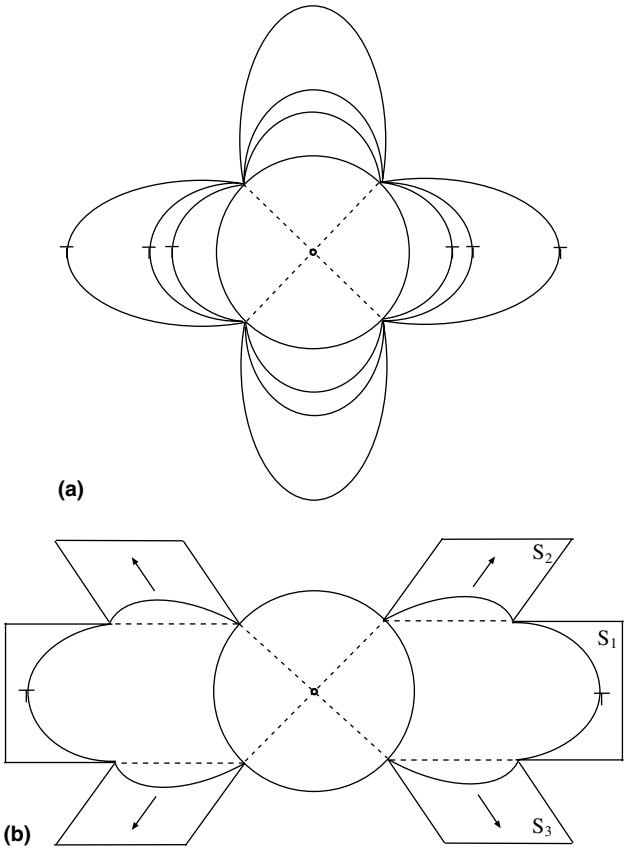


Fig. 7. Shear loop emission from void surface: (a) Top view of slip plane showing emission and propagation of several loops along four perpendicular directions; (b) Cross-slip of screw components of dislocations onto planes $S_2$ and $S_3$.

the average void size by an amount approximately equal to the magnitude of the dislocation Burgers vector (Fig. 8). Other arrangements, involving more that four pairs of dislocations, can also be envisioned as giving rise to the expansion of the void [47]. After the void has grown a finite amount, the network of sequentially emitted dislocations may appear as depicted in Fig. 9. In an analytical treatment of the void growth by dislocation emission, we consider the emission of a single dislocation and a single dislocation pair (prismatic or shear loop) from the surface of a cylindrical void under far-field biaxial tension. The critical stress required for the emission of both prismatic and shear loop is calculated as a function of the material properties and the initial size of the void. The analysis is based on the criterion adopted from a related study of the crack blunting by dislocation emission [48]. It is shown that the critical stress for the dislocation emission decreases with an increasing void size, so that less stress is required to emit dislocations from larger than smaller voids. At constant remote stress, this implies an accelerated void growth by continuing expulsion of prismatic and/or shear dislocation loops.

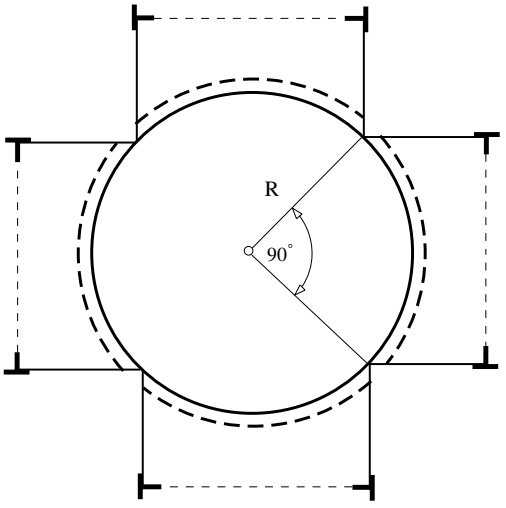


Fig. 8. Two-dimensional representation of four pairs of edge dislocations emitted from the surface of a cylindrical void giving rise to an increase of the average void radius by an amount approximately equal to the dislocation Burgers vector.

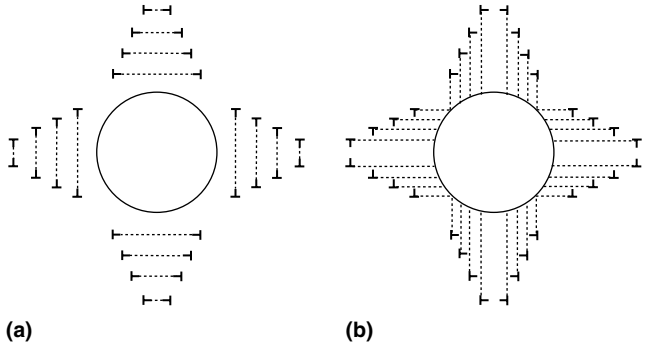


Fig. 9. After the void has grown a finite amount, the network of sequentially emitted dislocations may look as depicted in (a) for prismatic loops and (b) for shear loops.

## 5. Edge dislocation near a cylindrical void

The two-dimensional problem will be solved analytically. Consider an edge dislocation near a cylindrical void of radius $R$ in an infinitely extended isotropic elastic body. The dislocation is at the distance $d$ from the stress free surface of the void, along the slip plane parallel to the $x$-axis, as shown in Fig. 10(a). The stress and deformation fields for this problem have been derived by Dundurs and Mura [49]. The interaction energy between the dislocation and the void is

$$E_{\text{int}} = -\frac{Gb^2}{4\pi(1-\nu)}\left[\frac{x^2}{(x^2+y^2)^2} + \ln\frac{x^2+y^2}{x^2+y^2-R^2}\right], \quad y = \frac{R}{\sqrt{2}}, \tag{3}$$

where $b$ is the magnitude of the Burgers vector of the dislocation, $G$ is the elastic shear modulus, and $\nu$ is Poisson's ratio of the material. The dislocation is attracted by the surface of the void with the force

$$F_{\text{int}} = -\frac{\partial E_{\text{int}}}{\partial x} = \frac{Gb}{\pi(1-\nu)}\frac{b}{R}\frac{\xi(\xi^4+1/4)}{(\xi^2+1/2)^2(\xi^4-1/4)}, \quad \xi = \frac{x}{R}. \tag{4}$$

Suppose that a remote biaxial tension $\sigma$ is applied far from the void. Assuming the plane strain conditions, the radial, and circumferential stress components around the void are (e.g. [50])

$$\sigma_{\text{r}} = \sigma\left(1-\frac{R^2}{r^2}\right), \quad \sigma_\theta = \sigma\left(1+\frac{R^2}{r^2}\right). \tag{5}$$

The corresponding shear stress along the considered slip plane (Fig. 10(b)) is

$$\tau = \sqrt{2}\sigma\frac{\xi}{(\xi^2+1/2)^2}. \tag{6}$$

The total force on the dislocation (in the positive $x$-direction), due to the applied stress and the interaction with the void, is

$$F_x(\xi) = \sqrt{2}\sigma b\frac{\xi}{(\xi^2+1/2)^2} - \frac{Gb}{\pi(1-\nu)}\frac{b}{R}\frac{\xi(\xi^4+1/4)}{(\xi^2+1/2)^2(\xi^4-1/4)}. \tag{7}$$

The normalized force $F_x(\xi)/Gb$ vs. the normalized distance $d/b$ plot, where $d = x - R/\sqrt{2}$, is shown in Fig. 11, in the case when $R = 10b$, $\sigma = 0.07G$, and $\nu = 1/3$. The plot reveals an unstable equilibrium position of dislocation at $d \approx 2.11b$ and the mildly pronounced maximum force $F_{\max} \approx 0.012Gb$ at $d \approx 4.55b$. For $d$ smaller than $2.11b$, the dislocation is attracted to the void. In the limit $d/b \to \infty$ the dislocation force vanishes since the dislocation is far from the void, which finds itself in the field of uniform biaxial tension $\sigma$.

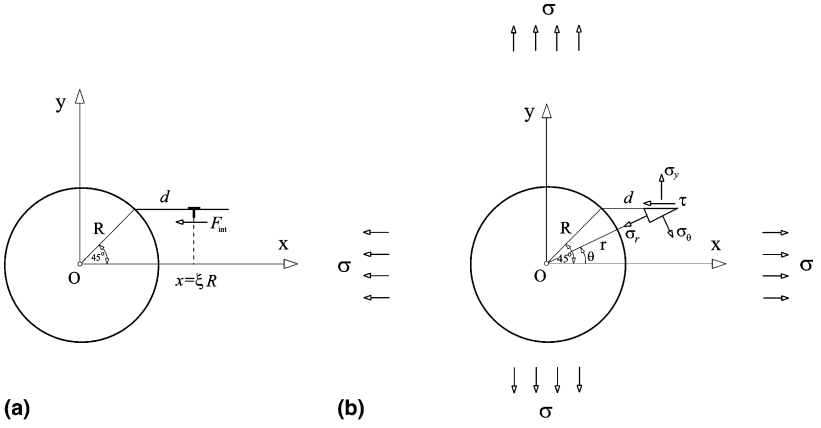


Fig. 10. (a) The edge dislocation at the distance $d$ from the stress free surface of the void. The dislocation slip plane is at distance $R/\sqrt{2}$ from the parallel $x$-axis. The radius of the void is $R$, and a non-dimensional variable $\xi = x/R$. The dislocation is attracted to the surface of the void by the force $F_{\text{int}}$. (b) The stress state at the point of the dislocation due to remote uniform tension $\sigma$. The shear stress along the slip plane toward the void is denoted by $\tau$.

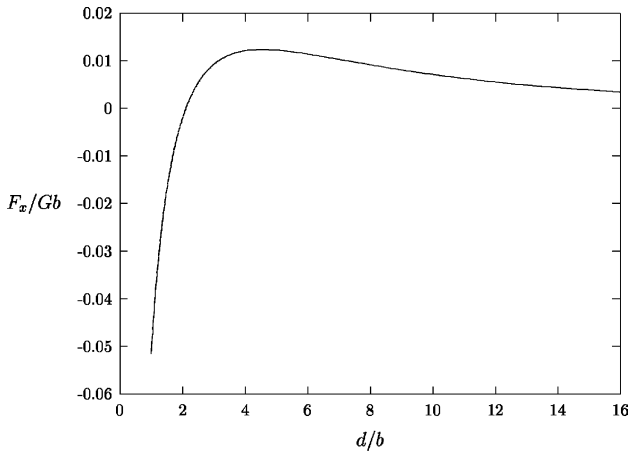


Fig. 11. The normalized dislocation force $F_x/Gb$ vs. the normalized distance from the void $d/b$, according to Eq. (7), in the case when $R = 10b$, $\sigma = 0.07G$, and $\nu = 1/3$. The dislocation is in an unstable equilibrium position at $d \approx 2.11b$.

## 6. An analysis of dislocation emission

In the equilibrium dislocation position, the attraction from the void is balanced by the applied stress, so that the force $F_x(\xi)$ in Eq. (7) vanishes, i.e.,

$$\sqrt{2}\sigma \frac{\xi}{(\xi^2+1/2)^2} = \frac{G}{\pi(1-\nu)} \frac{b}{R} \frac{\xi(\xi^4+1/4)}{(\xi^2+1/2)^2(\xi^4-1/4)}. \tag{8}$$

This gives

$$\xi^4 = \frac{1}{4} \frac{\sqrt{2}\pi(1-\nu)(\sigma/G)(R/b)+1}{\sqrt{2}\pi(1-\nu)(\sigma/G)(R/b)-1}. \tag{9}$$

Since

$$\xi = \frac{\sqrt{2}}{2} + \frac{d}{R}, \tag{10}$$

the equilibrium dislocation position is given by

$$d_{\rm cr} = \frac{R}{\sqrt{2}} \left\{ \left[ \frac{\sqrt{2}\pi(1-\nu)(\sigma/G)(R/b)+1}{\sqrt{2}\pi(1-\nu)(\sigma/G)(R/b)-1} \right]^{1/4} - 1 \right\}. \tag{11}$$

Adopting the criterion used by Rice and Thomson [48] for the spontaneous emission of dislocation from the crack tip, we propose that the dislocation will likely be emitted from the surface of the void if the equilibrium distance $d_{\rm cr}$ is less than the dislocation width (core cut-off) $w = \rho b$. Otherwise, there would be an energy barrier for a dislocation to overcome in order to arrive at the distance from the void greater than $w$. In the case of crack there is a large stress near the crack tip due to stress concentration, whereas in the case of the void under shock loading, the reflected shock pulse is of the order of $G/10$ ($\sim$5 GPa, Section 2), which may be sufficient to drive the dislocation out of the surface of the void. Thus, the condition for dislocation emission $d_{\rm cr} \leqslant w$ gives

$$\frac{R}{\sqrt{2}b} \left\{ \left[ \frac{\sqrt{2}\pi(1-\nu)(\sigma/G)(R/b)+1}{\sqrt{2}\pi(1-\nu)(\sigma/G)(R/b)-1} \right]^{1/4} - 1 \right\} \leqslant \rho. \tag{12}$$

If the radius of the void is given, this specifies the stress required to emit the dislocation

$$\frac{\sigma_{\rm cr}}{G} \geqslant \frac{b/R}{\sqrt{2}\pi(1-\nu)} \frac{(1+\sqrt{2}\rho b/R)^4+1}{(1+\sqrt{2}\rho b/R)^4-1}. \tag{13}$$

The plot of $\sigma_{\rm cr}/G$ vs. $R/b$ is shown in Fig. 12 for three selected values of the material parameter $\rho$ ($=1$, 1.5, and 2). The results are meaningful for sufficiently large sizes of voids, typically $R > 3\rho b$ ($R$ greater than $3b$ to $6b$). The critical stress required for dislocation emission decreases with both $\rho$ and $R/b$. The smaller the dislocation width, the higher the applied stress must be to keep the dislocation in equilibrium near the void. It is noted that the force on the dislocation at a given equilibrium distance from the void due to a remote stress increases more rapidly with the ratio $R/b$ than does the force due to attraction from the void surface. This is why the critical stress for dislocation emission decreases with increasing the $R/b$ ratio (i.e., the stress required to emit dislocation from a larger void is lower than from a smaller void). The limiting value of $\sigma_{\rm cr}$ for large voids ($b/R \to 0$) is

$$\lim_{b/R\to 0} \frac{\sigma_{\rm cr}}{G} = \frac{1}{4\pi(1-\nu)} \frac{1}{\rho}. \tag{14}$$

This also shows that the critical stress decreases with increasing dislocation width.

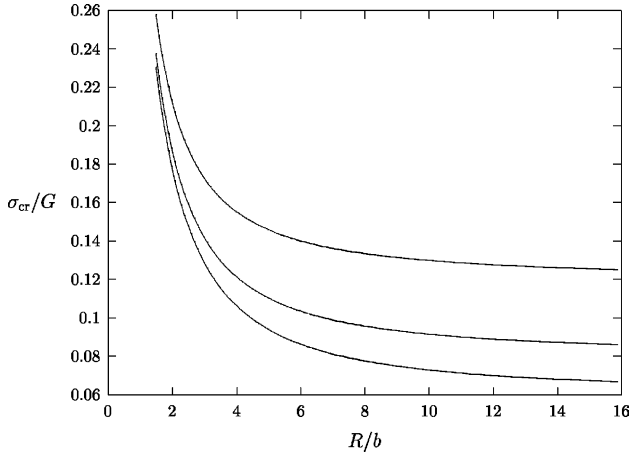


Fig. 12. The normalized critical stress $\sigma_{\rm cr}/G$ required to emit a dislocation from the surface of the void vs. the normalized radius of the void $R/b$, according to Eq. (13) with $\nu = 1/3$. The three curves correspond to three different sizes of dislocation width: the upper-most curve is for $\rho = 1$, the lower-most curve is for $\rho = 2$, and the middle curve is for $\rho = 1.5$.

The effect of the ledge left at the surface of the void behind the dislocation can also be included in the analysis. When the dislocation is far from the void, the ledge is fully formed with a width equal to the magnitude of the Burgers vector $b$. The corresponding increase of the energy is $\gamma b$, where $\gamma$ is the surface energy. When the dislocation is near the surface of the void, the ledge is only partially formed due to nearby dislocation core effects. Adopting the Peierls model of the dislocation, as in [48], when the dislocation is at the distance $d$ from the surface of the void, the width of the ledge left behind the dislocation is

$$\frac{2b}{\pi}\tan^{-1}\frac{2d}{e^{3/2}w}. \tag{15}$$

The core cut-off of the dislocation is $w=\rho b$ and $e$ is the Naperian logarithm base. Thus, the energy increase due to the creation of the ledge is

$$E_{\text{ledge}}=\frac{2\gamma b}{\pi}\tan^{-1}\frac{2d}{e^{3/2}w}. \tag{16}$$

The corresponding ledge force is

$$F_{\text{ledge}}=-\frac{\partial E_{\text{ledge}}}{\partial d}=-\frac{2\gamma}{\pi}\frac{\alpha}{\alpha^2+(d/b)^2},\quad \alpha=\frac{1}{2}e^{3/2}\rho \tag{17}$$

The total force on the dislocation is the sum of Eqs. (7) and (17). Numerical evaluations reveal that including the ledge force increases the critical stress for void growth. This increase is expected since the ledge increases the total energy of the system, creating an energy barrier for dislocation emission. For example, if $R/b=10$ and $\rho=2$, the ledge force increases the critical stress $\sigma_{\text{cr}}$ from $0.073G$ to $0.104G$. The performed calculations are for copper with $G=40$ GPa and a Burgers vector for $\{1\,1\,1\}\langle 1\,1\,0\rangle$ dislocation of magnitude $b=2.55$ Å. The value $\gamma=1.98$ J/m$^2$ for the surface energy of copper at $T=525$ °C was used. This value was obtained from the linear extrapolation $\gamma(T)=\gamma(T_0)+g(T-T_0)$ and the data reported by Murr [51]: $T_0=925$ °C, $\gamma(T_0)=1.78$ J/m$^2$, and $g=-0.0005$ J/m$^2$ °C. Numerical evaluations also reveal that the ledge effect on the critical stress is less pronounced for dislocations with a smaller dislocation width. For example, if $\rho=1.5$ is used in the above calculations, the ledge force increases the critical stress from $0.092G$ to $0.129G$. The ledge effect is more pronounced for smaller voids, because they exert weaker image forces by virtue of their smaller free surfaces.

More involved dislocation models, such as used by Rice [52] and Rice and Beltz [53] to study the crack blunting by dislocation emission, or by Xu and Argon [54] in their study of the homogeneous nucleation of dislocation loops in perfect crystals, may be needed to further improve the analysis of the void growth by dislocation emission. Experimental data in the literature (e.g. [55]) indicate that the spall strength of high purity Cu single crystals is about 5 GPa. The spall strength of a polycrystalline Cu is about half that value, because of grain boundaries and intercrystalline defects which promote void growth. Zurek and Meyers [56] and Meyers [57] discuss the effects of polycrystallinity and grain size on void growth during spall experiments and reconcile the contradictory results. The higher spall strength observed for monocrystalline copper is due to different nucleation sites. In polycrystals, there is segregation of impurities at the grain boundaries, providing favorable initiation sites. In monocrystals, these sites are absent and initiation has to occur from vacancy complexes.

## 7. Dislocation interaction effects

The calculation of the critical stress for void growth by dislocation emission is affected by the dislocation interaction. To elaborate, consider a pair of positive and negative dislocations shown in Fig. 13. An average increase of the void volume (per unit length in the $z$-direction) is equal to $\sqrt{2}Rb$. The dislocation force (directed toward the void) on the upper (negative) dislocation due to the lower (positive) dislocation is $F^{\text{d}}=b\tau^{\text{d}}$, where $\tau^{\text{d}}$ is the shear stress at the location of the negative dislocation exerted by the positive dislocation (Fig. 14(a)). This is

$$\tau^{\text{d}}=\tfrac{1}{2}\big(\sigma_u^{\text{d}}-\sigma_v^{\text{d}}\big)\sin 2\varphi-\sigma_{uv}^{\text{d}}\cos 2\varphi. \tag{18}$$

The stress components $\sigma_u^{\text{d}}$, $\sigma_v^{\text{d}}$, and $\sigma_{uv}^{\text{d}}$ can be determined from the Airy stress functions listed in Appendix A by using the following geometric specifications (see Fig. 14(b)):

$$r=\zeta R,\quad r_1=\sqrt{2}R,\quad r_2=\left(\zeta^2+\frac{1}{\zeta^2}-2\cos\theta\right)^{1/2}R, \tag{19}$$

and

$$\theta=2\varphi,\quad \theta_1=\varphi+\frac{\pi}{2},\quad \sin\theta_2=\frac{r_1}{r_2}\cos\varphi. \tag{20}$$

The angle $\varphi$ is defined in terms of the non-dimensional parameter $\xi=x/R$ by

$$\cos\varphi=\frac{\xi}{\zeta},\quad \zeta=\left(\xi^2+\frac{1}{2}\right)^{1/2}. \tag{21}$$

The $(u,v)$ coordinates of the point $B$ are

$$u=r\cos\theta=\frac{\zeta^2-1/2}{\zeta^2+1/2}R,\quad u_1=u-\zeta R,\quad u_2=u-\frac{R}{\zeta}, \tag{22}$$

and

$$v=v_1=v_2=r\sin\theta=\frac{\sqrt{2}\zeta^2}{\zeta^2+1/2}R. \tag{23}$$

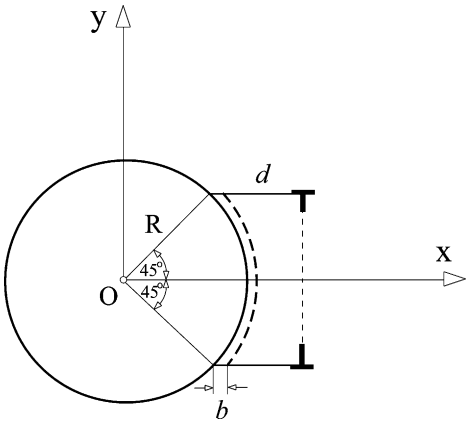


Fig. 13. A pair of opposite edge dislocations emitted from the surface of the void along two parallel slip planes cause the expansion of the segment of the void surface by the slip $b$ (magnitude of the dislocation Burgers vector).

The components of the Burgers vector of the dislocation at $A$ are $b_u = b\cos\varphi$ and $b_v = b\sin\varphi$. The total force on the dislocation at $B$, due to the applied stress $\sigma$ and the interaction with the surface of the void and the dislocation at $A$, is obtained by the superposition as

$$F_x(\xi) = \sqrt{2}\sigma b \frac{\xi}{(\xi^2+1/2)^2} - \frac{Gb}{\pi(1-\nu)}\frac{b}{R} \times \frac{\xi(\xi^4+1/4)}{(\xi^2+1/2)^2(\xi^4-1/4)} + b\tau^{\mathrm{d}}(\xi). \tag{24}$$

The plot of the normalized force $F_x/Gb$ vs. the normalized distance of the dislocation from the surface of the void $d/b$ is shown by the lower curve in Fig. 15, for the case when $R = 10b$, $\sigma = 0.07G$ and $\nu = 1/3$. The plot reveals an unstable equilibrium position of dislocation at $d \approx 2.62b$, and a mildly pronounced maximum force $F_{\max} \approx 0.00838Gb$ at $d \approx 4.97b$. There is also a stable equilibrium position at $d \approx 12.19b$. The upper curve in Fig. 15 shows the results obtained without incorporation of the dislocation interaction effects (same as in Fig. 11,

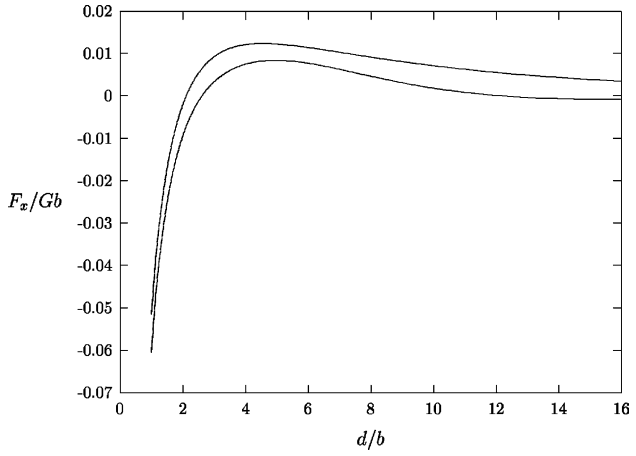


Fig. 15. The normalized dislocation force $F_x/Gb$ vs. the normalized distance from the void $d/b$ with the included dislocation interaction effects – lower curve, according to Eq. (24); and without dislocation interaction – upper curve, according to Eq. (7). The calculations are for $R = 10b$, $\sigma = 0.07G$, and $\nu = 1/3$. The dislocation is in an unstable equilibrium position at $d \approx 2.615b$. There is also a stable equilibrium position at $d \approx 12.185b$.

with the equilibrium dislocation position at $d \approx 2.11b$, and the maximum force $F_{\max} \approx 0.012Gb$ at $d \approx 4.55b$). The difference can be explained by observing that the shear stress $\tau^{\mathrm{d}}$ at $B$, shown in Fig. 14(a), due to dislocation at $A$ is negative and directed away from the void. The corresponding contribution to the force on the (negative) dislocation at $B$ is then directed toward the void. Consequently, the dislocation pair is in equilibrium at a larger distance from the surface of the void than is a single dislocation. Alternatively, this is a consequence of the fact that the dislocation pair is more strongly attracted to the surface of the void than a single dislocation.

In the equilibrium position, the dislocation force vanishes $F_x(\xi) = 0$. With $F_x(\xi)$ defined by Eq. (24), and for given $\sigma$ and $R$, this represents a highly nonlinear polynomial equation for $\xi$, which can be solved only numerically. Denoting the so determined value of $\xi$ by

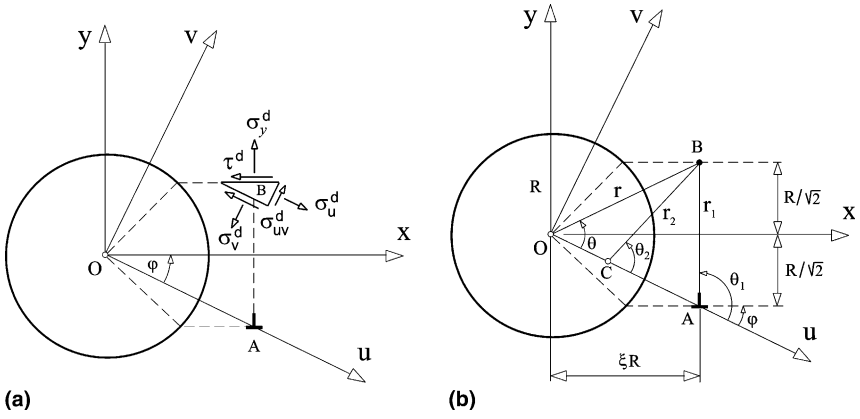


Fig. 14. (a) The shear stress $\tau^{\mathrm{d}}$ along the horizontal slip plane at the point $B$ associated with the stress field $\sigma_u^{\mathrm{d}}$, $\sigma_v^{\mathrm{d}}$, and $\sigma_{uv}^{\mathrm{d}}$ of the edge dislocation at the point $A$. (b) The geometric quantities appearing in the expressions for the stress components at the point $B$ due to edge dislocation at the point $A$. The lengths $\overline{OA} = \overline{OB} = r = \zeta R$, $\overline{OC} = R/\zeta$, $\overline{AB} = r_1$, and $\overline{CB} = r_2$. The angle $\varphi = \theta/2$.

$\xi_{cr}$, the corresponding unstable equilibrium dislocation position is

$$d_{cr} = \left(\xi_{cr} - \frac{1}{\sqrt{2}}\right)R. \tag{25}$$

On the other hand, if we want to find the critical stress $\sigma_{cr}$ for the emission of the dislocation pair from the surface of the void (Fig. 13), we require that $d_{cr}$ is equal (or less) than the dislocation width $w = \rho b$, i.e., $d_{cr} = \rho b$. Combining this with Eq. (25) gives

$$\xi_{cr} = \frac{1}{\sqrt{2}} + \rho\frac{b}{R}. \tag{26}$$

The substitution into Eq. (24), in conjunction with $F_x(\xi) = 0$, delivers the critical stress

$$\sigma_{cr} = \frac{G}{\sqrt{2}\pi(1-\nu)}\frac{b}{R}\frac{\xi_{cr}^4 + 1/4}{\xi_{cr}^4 - 1/4} - \frac{(\xi_{cr}^2 + 1/2)^2}{\sqrt{2}\xi_{cr}}\tau^{d}(\xi_{cr}). \tag{27}$$

The plot of $\sigma_{cr}/G$ vs. $R/b$ is shown in Fig. 16 for the case when the parameter $\rho = 1$ (upper curve). The lower curve shows the previously calculated results from Fig. 12 for the emission of a single dislocation. Clearly, regardless of the size of the void, higher stress is needed to emit a dislocation pair than to emit a single dislocation. For example, for $R/b = 10$, the ratio $\sigma_{cr}/G$ is equal to 0.14 in the first case, and to 0.13 in the second case. By incorporating the ledge effect (discussed at length in Section 6), the critical stress for the emission of dislocations increases. For example, if $R/b = 10$ and $\rho = 2$, the critical stress is $\sigma_{cr} = 0.114G$, as compared to $0.083G$ without the ledge effect.

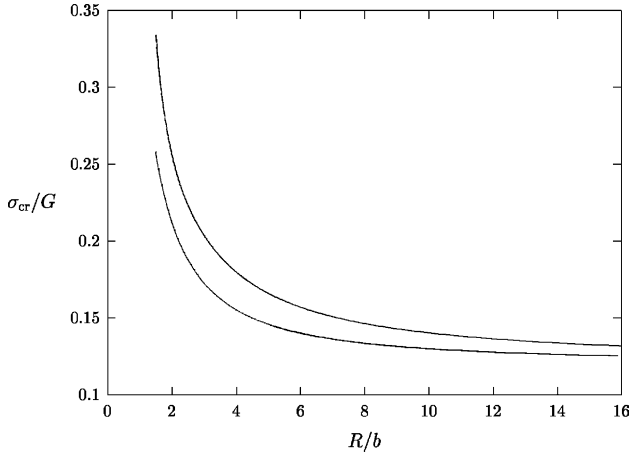


Fig. 16. The normalized critical stress $\sigma_{cr}/G$ required to emit the dislocation from the surface of the void vs. the normalized radius of the void $R/b$. The upper curve corresponds to emission of the dislocation pair, according to Eq. (27); the lower curve is for the single dislocation, according to Eq. (13). The calculations are for $\rho = 1$ and $\nu = 1/3$.

## 8. Conclusions

Experiments providing extreme conditions of high tensile stress (~5 GPa) and low durations (~10 ns) were conducted using high-power lasers as the energy deposition source. These experiments yielded voids with diameters up to 10 μm (a radial expansion velocity of approximately $10^3$ m/s). It is shown that vacancy diffusion cannot account for growth at these strain rates. A combined mechanics-materials approach to void growth under dynamic loading conditions, in which the process of dislocation emission prevails over the diffusion or creep mechanism of the void growth, is of great significance for better understanding of the dynamic strength of materials and the formulation of the corresponding failure criteria. Toward this goal, we developed in this paper an analysis of the void growth by dislocation emission. A criterion for the emission of dislocation from the surface of the void is formulated, which is analogous to Rice and Thomson's criterion [48] for crack blunting by dislocation emission from the crack tip. A two-dimensional model is considered with emission of edge dislocations from the surface of a cylindrical void. The critical stress required to emit a single dislocation and a dislocation pair under remote biaxial tension is calculated. It is shown that the critical stress for dislocation emission decreases with an increasing void size, so that less stress is required to emit dislocations from larger than smaller voids. At a constant remote stress, this implies an accelerated void growth by continuing expulsion of prismatic or shear dislocation loops. It is also found that dislocations with a wider dislocation core are more easily emitted than dislocations with a narrow dislocation core.

## Acknowledgements

The authors are grateful for the research support provided by the Department of Energy (Grant DE-FG03-98DP00212) and discussions with J. Belak of Lawrence Livermore National Laboratory. The authors also thank the National Center for Electron Microscopy for use of their transmission electron microscope facilities. The help of Dr. Fabienne Gregori (University of Paris 13) with the transmission electron microscopy work is gratefully acknowledged.

## Appendix A. Stresses due to edge dislocation near a void

The stress components at the point $B$ due to edge dislocation with the Burgers vector $\mathbf{b} = \{b_u, b_v\}$ at the point $A$ near the circular void of radius $R$ (Fig. 14) can be calculated from the results derived by Dundurs and Mura [49] and Dundurs [58]. The Airy stress functions for the two dislocation components are:

$$\chi^{b_u} = -\frac{Gb_u}{2\pi(1-\nu)}\left[r_1\ln r_1\sin\theta_1 - r_2\ln r_2\sin\theta_2 + r\ln r\sin\theta + \frac{\zeta^2-1}{2\zeta^3}R\sin 2\theta_2 - \frac{(\zeta^2-1)^2}{\zeta^4}\frac{R^2}{2r_2}\sin\theta_2 + \frac{R^2}{2r}\sin\theta\right], \tag{A.1}$$

$$\chi^{b_v} = \frac{Gb_v}{2\pi(1-\nu)}\left[r_1\ln r_1\cos\theta_1 - r_2\ln r_2\cos\theta_2 + r\ln r\cos\theta - \frac{\zeta^2-1}{\zeta}R\ln r + \frac{\zeta^2-1}{\zeta}R\ln r_2 - \frac{\zeta^2-1}{2\zeta^3}R\cos 2\theta_2 + \frac{(\zeta^2-1)^2}{\zeta^4}\frac{R}{2r_2}\cos\theta_2 + \frac{R^2}{2r}\cos\theta\right]. \tag{A.2}$$

The shear modulus and Poisson's ratio of the material are $G$ and $\nu$, and a non-dimensional parameter $\zeta = \overline{OA}/R$ defines the position of dislocation relative to the void. The stresses are derived from the stress function $\chi = \chi^{b_u} + \chi^{b_v}$ as

$$\sigma_u = \frac{\partial^2\chi}{\partial v^2}, \quad \sigma_v = \frac{\partial^2\chi}{\partial u^2}, \quad \sigma_{uv} = -\frac{\partial^2\chi}{\partial u\,\partial v}. \tag{A.3}$$

The resulting expressions are incorporated in the computer program for calculating the critical stress for dislocation pair emission used in Section 7.

## References


[1] Meyers MA, Aimone CT. Progr Mater Sci 1983;28:1.
[2] Meyers MA, Murr LE, editors. Metallurgical effects of shock waves and high-strain-rate phenomena in metals. New York: Plenum; 1981.
[3] Worswick MJ, Pick RJ. Mech Mater 1995;19:293.
[4] McClintock FA. J Appl Mech 1968;35:363.
[5] Rice JR, Tracey DM. J Mech Phys Solids 1969;17:201.
[6] Needleman A. J Appl Mech 1972;39:964.
[7] Hellan K. Int J Mech Sci 1975;17:369.
[8] Gurson AL. J Engng Mater Technol 1977;99:2.
[9] Goods SH, Brown LM. Acta Metall 1979;27:1.
[10] Budiansky B, Hutchinson JW, Slutsky S. In: Hopkins HG, Sewell MJ, editors. Mechanics of solids: the Rodney Hill 60th anniversary volume. Oxford: Pergamon Press; 1982. p. 13–45.
[11] Nemat-Nasser S, Hori M. J Appl Phys 1987;62:2746.
[12] Chung D-T, Horgan CO, Abeyaratne R. Int J Solids Struct 1987;23:983.
[13] Koplik J, Needleman A. Int J Solids Struct 1988;24:835.
[14] Kameda J. Acta Metall 1989;37:2067.
[15] Tvergaard V. Adv Appl Mech 1990;27:83.
[16] Huang Y, Hutchinson JW, Tvergaard V. J Mech Phys Solids 1991;39:223.
[17] Needleman A, Tvergaard V, Hutchinson JW. In: Argon AS, editor. Fracture and fatigue. New York: Springer-Verlag; 1992. p. 145–78.
[18] Cuitiño AM, Ortiz M. Acta Mater 1996;44:427.
[19] Plekhanov PS, Gösele UM, Tan TY. J Appl Phys 1998;84:718.
[20] Pardoen T, Hutchinson JW. J Mech Phys Solids 2000;48:2467.
[21] Kassner ME, Hayes TA. Int J Plasticity 2003;19:1715.
[22] Hopkins HG. In: Sneddon IN, Hill R, editors. Progress in solid mechanics, vol. 1. Groningen: North-Holland; 1960. p. 81–164.
[23] Carroll MM, Holt AC. J Appl Phys 1972;43:1626.
[24] Johnson JN. J Appl Phys 1981;52:2812.
[25] Cortés R. Int J Solids Struct 1992;29:1637.
[26] Ortiz M, Molinari A. J Appl Mech 1992;59:48.
[27] Benson DJ. J Mech Phys Solids 1993;41:1285.
[28] Wang ZP. Int J Solids Struct 1994;31:2139.
[29] Wu XY, Ramesh KT, Wright TW. J Mech Phys Solids 2003;51:1.
[30] Williams ML, Schapery RA. Int J Fract Mech 1965;1:64.
[31] Ball JM. Philos Trans R Soc Lond 1982;A306:557.
[32] Stuart CA. Ann Inst Henri Poincaré-Analyse non linéaire 1985;2:33.
[33] Horgan CO. Int J Solids Struct 1992;29:279.
[34] Polignone DA, Horgan CO. Int J Solids Struct 1993;30:3381.
[35] Horgan CO. Polignone DA. Appl Mech Rev 1996;48:471.
[36] Stevens L, Davison L, Warren WE. J Appl Phys 1972;42:4922.
[37] Belak J. In: Schmidt SC, Dandekar DP, Forbes JW, editors. Shock Compression of Condensed Matter – 1997, AIP Conference Proceedings, vol. 429. Woodbury: American Institute of Physics Press; 1998. p. 211.
[38] Rudd RE, Belak JF. Comp Mater Sci 2002;24:148.
[39] Meyers MA, Gregori F, Kad BK, Schneider MS, Kalantar DH, Remington BA, Ravichandran R, Boehly T, Wark JS. Acta Mater 2003;51:1211.
[40] Kalantar DH, Belak J, Bringa E, Budil K, Caturla M, Colvin J, et al. J Plasma Phys 2003;10:1569.
[41] Christy S, Pak HR, Meyers MA. In: Meyers MA, Murr LE, Staudhammer KP, editors. Shock-wave and high-strain-rate phenomena in materials. New York; 1986 p. 835–63.
[42] Balluffi RW, Granato AV. In: Nabarro FRN, editor. Dislocations in solids, vol. 4. New York: North-Holland; 1979. p. 26–7.
[43] Kressel H, Brown N. J Appl Phys 1967;38:138.
[44] Meyers MA. In: Dynamic behavior of materials. New York: Wiley; 1994. p. 415–20.
[45] Takamura J-I. In: Cahn RW, editor. Physical metallurgy. Amsterdam: North-Holland; 1970. p. 857–920.
[46] Ashby MF. Philos Mag 1970;21:399.
[47] Hahn GT, Flanagan WF. In: Ashby MF, Bullough R, Hartley CS, Hirth JP, editors. Dislocation modelling of physical systems. Oxford: Pergamon Press; 1980. p. 1–17.
[48] Rice JR, Thomson R. Philos Mag A 1974;29:73.
[49] Dundurs J, Mura T. J Mech Phys Solids 1964;12:177.
[50] Timoshenko S, Goodier JN. Theory of elasticity. New York: McGraw-Hill; 1970. p. 70.
[51] Murr LE. In: Interfacial phenomena in metals and alloys. Reading, MA: Addison-Wesley; 1975. p. 124.
[52] Rice JR. J Mech Phys Solids 1992;40:239.
[53] Rice JR, Beltz GE. J Mech Phys Solids 1994;42:333.
[54] Xu G, Argon AS. Philos Mag Lett 2000;80:605.
[55] Minich RW, Kumar M, Cazamia J, Schwartz AJ. Dynamic Deformation: Constitutive Modeling, Grain Size, and Other Effects. 2003 TMS Annual Meeting, San Diego; 2003.
[56] Meyers MA, Zurek AK. In: Davison L, Grady DE, Shahinpoor M, editors. High pressure shock compression of solids II. New York: Springer; 1996. p. 25–70.
[57] Meyers MA. In: Meyers MA, Armstrong RW, Kirchner HOK, editors. Mechanics and materials: fundamentals and linkages. Amsterdam: Elsevier; 1999. p. 489–594.
[58] Dundurs J. In: Mura T, editor. Mathematical theory of dislocations. New York: ASME; 1969. p. 70–115.